DIGITAL IMPLEMENTATION OF NON-INTEGER CONTROL AND ITS APPLICATION TO A TWO-LINK ROBOTIC ARM

Duarte Valério*; José Sá da Costa*
* Technical University of Lisbon, Instituto Superior Técnico
Department of Mechanical Engineering, GCAR
Av. Rovisco Pais, 1049-001 Lisboa, Portugal
Phone: +351 21 8417187 Fax +351 21 8498097
Email: {dvalerio;sadacosta}@dem.ist.utl.pt

Keywords: Non-integer order control; position / force hybrid control; CRONE; digital control; robot.

Abstract

This paper assesses relative merits and drawbacks of different digital implementations of non-integer order controllers. Twenty-eight formulas are considered. Their frequency behaviours, together with those of discretised CRONE controllers, are compared to the ideal ones. All those formulas are used for implementing controllers found in the literature for a robotic arm. Backward finite difference formulas, Tustin formula and a zero order hold discretisation of a CRONE controller achieve the best results.

1 Introduction

The application of non-integer calculus to the field of control has resulted in controllers with good robustness properties that may be applied to the control of robots. This is a demanding area, where performance specifications often call for an accurate control. This is particularly the case of hybrid control, where both the position of the robot actuator and the force it exerts on a surface must be taken into account.

This paper is organised as follows. Section 2 introduces different formulas for implementing approximations of a non-integer order derivative in the time domain. Section 3 presents the application of these formulas to the position / force hybrid control of a robot. Section 4 draws some conclusions.

2 Formulas for discrete-time implementation

This section deals with how to implement a transfer function $G(s)=s^v$, $v\in\mathbb{R}$, in the time domain.

2.1 MacLaurin expansion formulas

Grünwald-Letnikoff or first-order backward finite difference formula. Operator D may be implemented in the time-domain by using the Grünwald-Letnikoff definition of a non-integer order derivative $D^v y(t)$, $v\in\mathbb{R}$:

$$D^v y(t) = \lim_{h\to 0}\frac{1}{h^v}\sum_{k=0}^{+\infty}\frac{(-1)^k\,\Gamma(v+1)}{\Gamma(k+1)\Gamma(v-k+1)}y(t-kh) \qquad (1)$$

Time-step h will be approximated by the sampling time T, and the summation will be truncated after a finite number of terms n [3], resulting in formula (12) of Table 2. This formula might also have been obtained from a first-order backward finite difference $(1-z^{-1})/T$. Raising the finite difference to a non-integer power v results in something which is *not* the ratio of two polynomials in z^{-1}. But performing a MacLaurin series expansion (which is reasonable since sampling times ought to be small), we will obtain a polynomial in z^{-1}:

$$D^v y(t) \approx \left(\frac{1-z^{-1}}{T}\right)^v y(t) = \frac{y(t)}{T^v}\left[\sum_{i=0}^{+\infty}\frac{(-1)^i\,\Gamma(v+1)z^{-i}}{\Gamma(i+1)\Gamma(v-i+1)}\right] \qquad (2)$$

(See the Appendix on how expansions found throughout the paper have been obtained.) This polynomial, truncated after n terms (this is needed since the MacLaurin series has an infinite number of terms), results in formula (12) again.

Second and third order backward finite difference formulas. It is reasonable to try to use higher-order finite differences, in the same manner as a first-order one was, for approximating operator D [5]. The results for second-order and third-order backward finite differences are given in Table 2.

Tustin and Simpson formulas. Instead of approximating derivatives with finite differences, other formulas for conversion between the continuous and discrete domains may be used [3, 5]. Results for Tustin and Simpson formulas are given in Table 2.

2.2 Impulse and step response formulas

Two further formulas for approximating operator D may be obtained requiring the impulse response or the step response to be equal, at sampling times, to the ideal impulse or step responses, respectively. This, however, is not feasible for t=0, since these responses are not always continuous at that instant. An additional condition is needed for determining the independent coefficient of the transfer function; the choice was to require both the impulse and the step responses to be equal to the ideal ones at $t=T_s$; for further time instants only one of those two responses is to be followed. The two resulting formulas are given in Table 2.

2.3 Continued fraction expansion formulas

We have now seven formulas for implementing approximations of non-integer order derivatives in the time domain, five of which include a truncated MacLaurin series expansion, which was necessary for providing a polynomial approximation of a non-rational quantity.

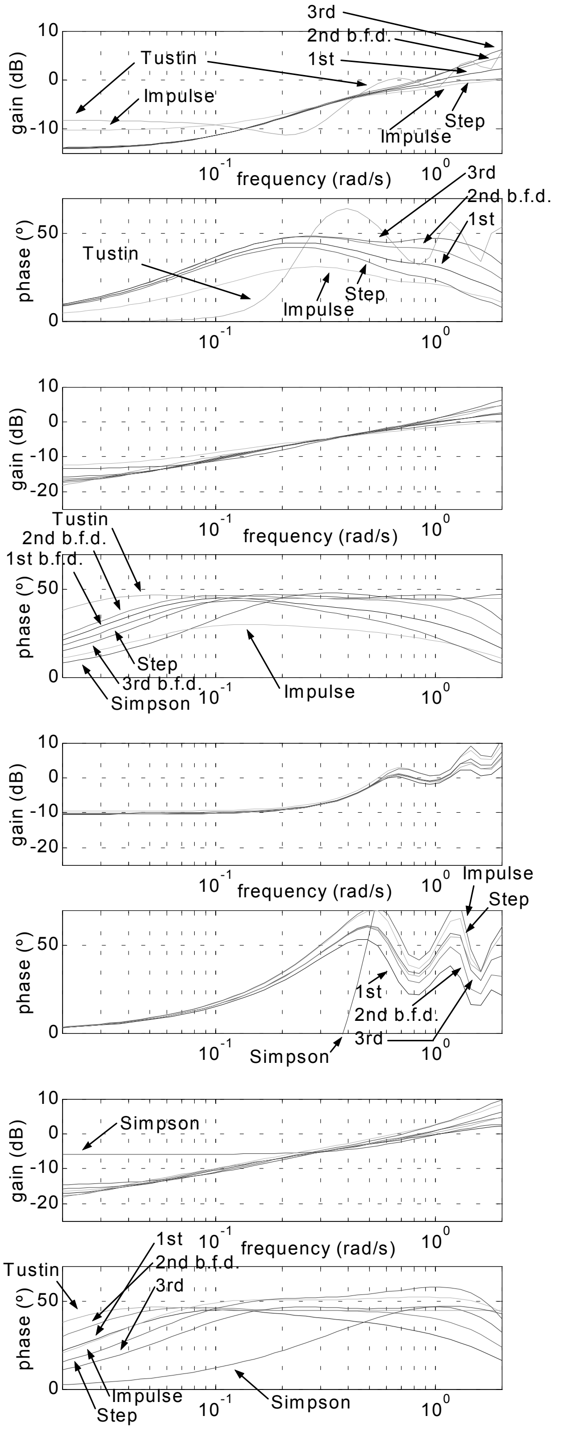

Figure 1. Bode diagrams for a 0.5 derivative implemented with n=9 for a sampling time of 1 s; from top to down: formulas of Table 2; formulas of Table 1; formulas of Table 2 inverted with (3); formulas of Table 1 inverted with (3)

Instead of a MacLaurin series expansion a continued fraction expansion can be used (this is done in [6] for the first order backward finite difference and Tustin formulas). In impulse and time response formulas no expansions appear: nevertheless, it is possible to expand the corresponding series into a continued fraction. Seven additional formulas for implementing non-integer derivatives in the time domain, found in Table 1, will thus be obtained.

2.4 Inverted formulas

All formulas presented so far are approximations of a non-integer power of the Laplace variable s. As $s=1/s^{-1}$, it is possible to write

$$D^{v}y(t)=\frac{1}{D^{-v}y(t)} \tag{3}$$

Applying expression (3) to the formulas of Table 1 and Table 2 results in fourteen additional formulas for implementing D (this is done in [6] for the first order backward finite difference formula). This is important since some formulas may have good performances for positive values of v but not for negative ones, or vice-versa: expression (3) allows choosing the sign with which results will be better.

2.5 Discretised frequency-domain non-integer controllers

Several frequency-domain approximations of non-integer controllers are described in the literature, of which the CRONE is the best known [4]. These may be discretised in the usual ways.

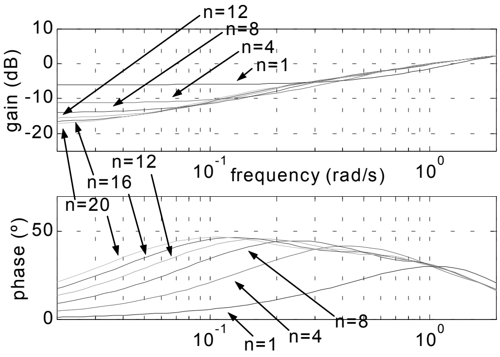

Figure 2. Bode diagrams for a 0.5 derivative implemented with formula (12) for a sampling time of 1 s

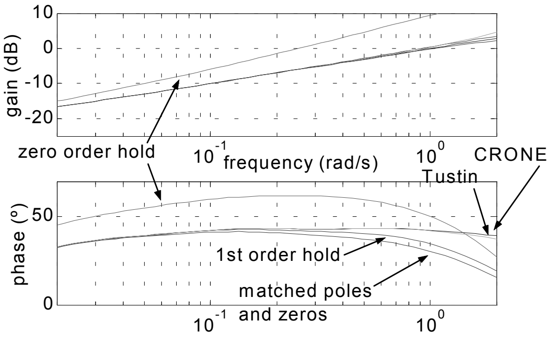

Figure 3. Bode diagrams of discretisations of (4)

2.6 Bode diagrams

Computing the gain and the phase of $G(s)=s^{v}$ shows that its Bode diagram has a constant $v\pi/2$ rad phase and a linear gain with a $20v$ dB/decade slope. Different formulas approximate this ideal Bode diagram in a limited frequency range, as seen in Figure 1 for v=0.5 (in which case the phase should be $0.5\pi/2$ rad = 45º, and the gain should have a slope of

20×0.5=10 dB/decade). In what concerns formulas of Table 2, the best approximations are given by (in decreasing order) third, second and first order backward finite difference formulas, step and impulse response formulas. Tustin formula results in a Bode diagram with spurious oscillations and Simpson formula has a Bode plot that is completely out of range. In what concerns formulas of Table 1, all achieve a reasonable approximation, impulse response formula being the worst (well behind Simpson formula, this time). When formulas of Table 2 are inverted with formula (3) spurious oscillations appear: this shows that those inverted formulas should not be used for positive values of *v*, but only for negative ones. When formulas of Table 1 are inverted with formula (3) all achieve a reasonable approximation, Simpson formula resulting now in the poorest performance.

The number of terms kept after the truncation is also of importance: as seen in Figure 2 for the first order backward finite difference formula, increasing *n* improves the performance especially for low frequencies.

A comparison with a discretised CRONE controller must be carried out using a similar number of zeros and poles and a similar frequency range. Controllers of Figure 1 having good results in the [0.1;1] rad/s range, a CRONE controller with similar performance will be

$$\frac{3.15s^4+10.48s^3+5.241s^2+0.442s+0.005601}{s^4+7.89s^3+9.356s^2+1.871s+0.05623} \tag{4}$$

Discretisations thereof, as seen in Figure 3, provide good approximations of the ideal Bode diagram, the best method of discretisation being Tustin, and the poorest zero order hold.

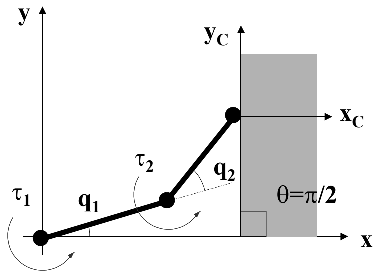

Figure 4. Robotic arm

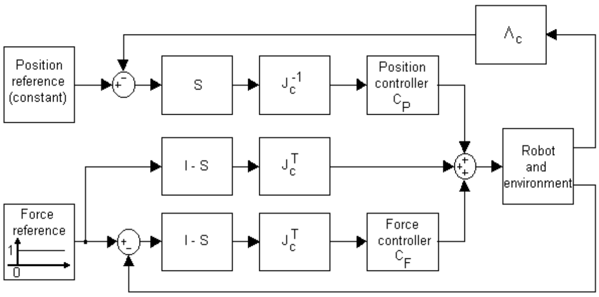

Figure 5. Control scheme

3 Control of a robot arm

In this section formulas presented above are applied to a plant found in the literature [2] to which non-integer order control has been successfully applied. The purpose is to verify relative merits and drawbacks of different implementations.

3.1 Description

Let us consider a 2D robotic arm with two degrees of freedom consisting of two rigid links (with masses m_1 and m_2, lengths r_1 and r_2, moments of inertia $J_{1\mathrm{m}}$ and $J_{2\mathrm{m}}$, and connected by joints with moments of inertia $J_{1\mathrm{g}}$ and $J_{2\mathrm{g}}$), leaning on a surface as seen in Figure 4. Its dynamic behaviour is given by

$$\boldsymbol{\tau}=\mathbf{H}(\mathbf{q})\ddot{\mathbf{q}}+\mathbf{c}(\mathbf{q},\dot{\mathbf{q}})+\mathbf{g}(\mathbf{q})-\mathbf{J}^T(\mathbf{q})\mathbf{F}$$

$$\begin{cases}\mathbf{H}_{11}(\mathbf{q})=(m_1+m_2)r_1^2+m_2r_2^2+2m_2r_1r_2\cos(q_2)+J_{1m}+J_{1g}\\ \mathbf{H}_{12}(\mathbf{q})=m_2r_2^2+m_2r_1r_2\cos(q_2)\\ \mathbf{H}_{21}(\mathbf{q})=m_2r_2^2+m_2r_1r_2\cos(q_2)\\ \mathbf{H}_{22}(\mathbf{q})=m_2r_2^2+J_{2m}+J_{2g}\end{cases}$$

$$\mathbf{c}(\mathbf{q},\dot{\mathbf{q}})=\begin{bmatrix}-m_2r_1r_2\sin(q_2)\dot{q}_2^2-2m_2r_1r_2\sin(q_2)\dot{q}_1\dot{q}_2\\ m_2r_1r_2\sin(q_2)\dot{q}_1^2\end{bmatrix} \tag{5}$$

$$\mathbf{g}(\mathbf{q})=\begin{bmatrix}g\left(m_1r_1\cos(q_1)+m_2r_1\cos(q_1)+m_2r_2\cos(q_1+q_2)\right)\\ gm_2r_2\cos(q_1+q_2)\end{bmatrix}$$

$$\begin{cases}\mathbf{J}_{11}(\mathbf{q})=-r_1\sin(q_1)-r_2\sin(q_1+q_2)\\ \mathbf{J}_{21}(\mathbf{q})=r_1\cos(q_1)+r_2\cos(q_1+q_2)\\ \mathbf{J}_{12}(\mathbf{q})=-r_2\sin(q_1+q_2)\\ \mathbf{J}_{22}(\mathbf{q})=r_2\cos(q_1+q_2)\end{cases}$$

where $\mathbf{q}=[q_1\ q_2]^\mathrm{T}$ is a 2×1 vector of joint coordinates, as seen in Figure 4; $\tau=[\tau_1\ \tau_2]^\mathrm{T}$ is a 2×1 vector of actuator torques, consisting of the torques applied to each of the two joints; $\mathbf{H}(\mathbf{q})$ is a 2×2 inertia matrix,; $\mathbf{c}(\mathbf{q},\dot{\mathbf{q}})$ is a 2×1 vector of centrifugal and Coriolis terms; $\mathbf{g}(\mathbf{q})$ is a 2×1 vector of gravitational terms; $\mathbf{J}(\mathbf{q})$ is the 2×2 Jacobian matrix of the robot; and $\mathbf{F}$ is a 2×1 vector with the force exerted by the environment on the robot's tip, which, the wall against which the robot leans being vertical and friction being neglected, will be modelled by

$$\mathbf{F}=\begin{bmatrix}M\ddot{x}_c+B\dot{x}_c+Kx_c\\ 0\end{bmatrix} \tag{6}$$

Coordinates *x* and *y* will be force and position controlled, respectively; the hybrid control scheme is found in Figure 5 [1]. The selection matrix **S**, the kinematic equations Λ_c (for finding $(x_\mathrm{c},y_\mathrm{c})$ from the joint coordinates (q_1,q_2)) and the Jacobian of these kinematic equations $\mathbf{J}_\mathrm{c}$ are given by

$$\mathbf{S}=\begin{bmatrix}0&0\\0&1\end{bmatrix},\quad \boldsymbol{\Lambda}_c:\begin{cases}x_c=r_1\sin(\theta-q_1)+r_2\sin(\theta-q_1-q_2)\\ y_c=r_1\cos(\theta-q_1)+r_2\cos(\theta-q_1-q_2)\end{cases}$$

$$\begin{cases}\mathbf{J}_{c11}(\mathbf{q})=-r_1\cos(\theta-q_1)-r_2\cos(\theta-q_1-q_2)\\ \mathbf{J}_{c12}(\mathbf{q})=-r_2\cos(\theta-q_1-q_2)\\ \mathbf{J}_{c21}(\mathbf{q})=r_1\sin(\theta-q_1)+r_2\sin(\theta-q_1-q_2)\\ \mathbf{J}_{c22}(\mathbf{q})=r_2\sin(\theta-q_1-q_2)\end{cases} \tag{7}$$

Robot and environment parameters are given in Table 3. A test will be performed with the robot beginning at $q_1=q_2=15\pi/36$, without exerting force on the environment; a 1 N step at the force reference is applied when $t=0$, while the vertical position y_c should remain constant.

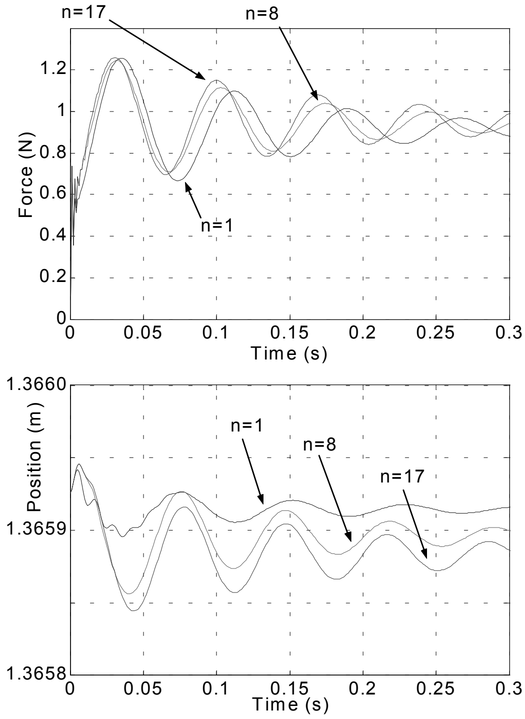

Figure 6. Effect of *n* for the first order backward finite difference formula

3.2 Non-integer order control

Non-integer order controllers given in the literature quoted above are $C_F=[10^3D^{-1/5}\;\;10^3D^{-1/5}]^T$ and $C_P=[10^5D^{1/2}\;\;10^5D^{1/2}]^T$, implemented with first order backward finite difference formula, n=17 and a sampling time of 1 ms. In what follows n=8, because a large n results in a larger steady-state error for the vertical position, in slightly larger overshoots for the force and in larger settling times. The value of n used here is a compromise with a smaller steady-state error for the force. This may be seen in Figure 6.

Only backward finite differences and Tustin formulas result in implementations that stabilize the control loop (third-order backward finite difference formula only if a MacLaurin series is used). Stable responses are shown in Figure 7. Inversion with (3) results in very similar force responses. Formulas given in Table 1 have larger transient responses and larger overshoots. The best force response is obtained with first order backward finite difference formula, using a MacLaurin expansion without inversion with (3) (formula (12)); Tustin formula, using a MacLaurin expansion without inversion with (3) (formula (15)), provides the best position response: but no clear advantage over other MacLaurin expanded stability-achieving implementations exists.

CRONE controllers reckoned for the [100,1000] rad/s frequency range and having a similar number of zeros and poles are

$$C_F=\frac{398.6s^4+4.502\times10^6s^3+5.219\times10^9s^2+\ldots+3.021\times10^{11}s+6.318\times10^{12}}{s^4+9530s^3+8.261\times10^6s^2+7.126\times10^8s+6.31\times10^9}\qquad(8)$$

$$C_P=\frac{3.157\times10^6s^4+1.05\times10^{10}s^3+5.252\times10^{12}s^2+\ldots+4.429\times10^{14}s+5.613\times10^{15}}{s^4+7890s^3+9.356\times10^6s^2+1.871\times10^9s+5.623\times10^{10}}$$

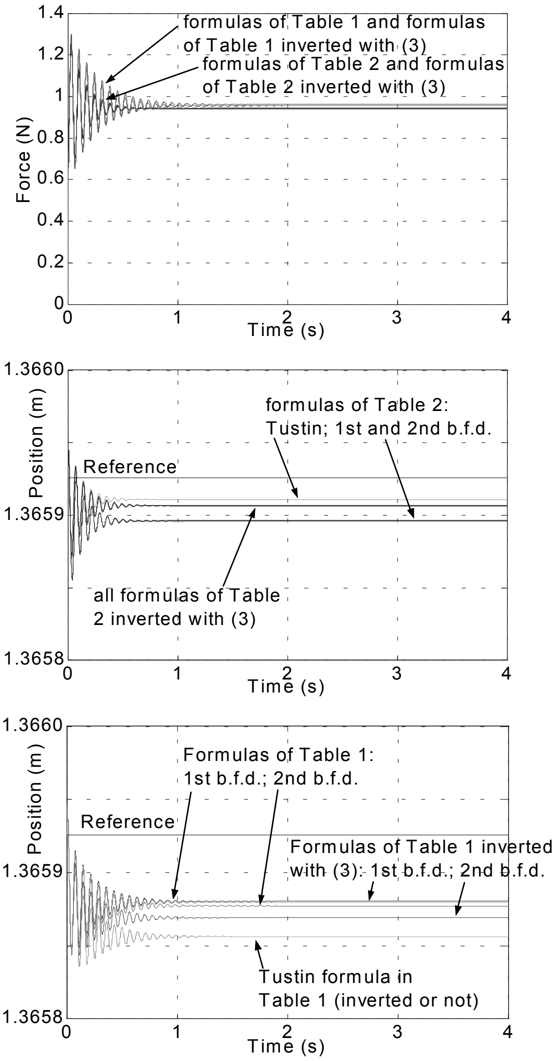

Figure 7. Performance of different formulas

Only a zero-order hold discretisation thereof achieves a stable control loop, with, as seen in Figure 8, a very good result in what concerns force control (the best in this paper), but a very poor one in what concerns position control.

4 Conclusions

The following conclusions may be drawn:

❖ backward finite differences formulas provide good approximations of *D* in the discrete time domain (with the exception of the third order backward finite difference formula expanded into a continued fraction);

❖ both MacLaurin series and continued fraction expansions may be used; the latter have Bode diagrams closer to the ideal ones, but poorer results when non-integer order controllers for a robot were simulated;

- ❖ Tustin formula approximations have Bode diagrams not always close to the ideal ones, but perform well in the simulations of the robotic arm;
- ❖ Simpson, impulse response and step response formulas provide unacceptable results;
- ❖ discretised CRONE controllers have Bode diagrams close to the ideal one, but only a zero-order hold discretisation had a good performance when simulating the control of the robot.

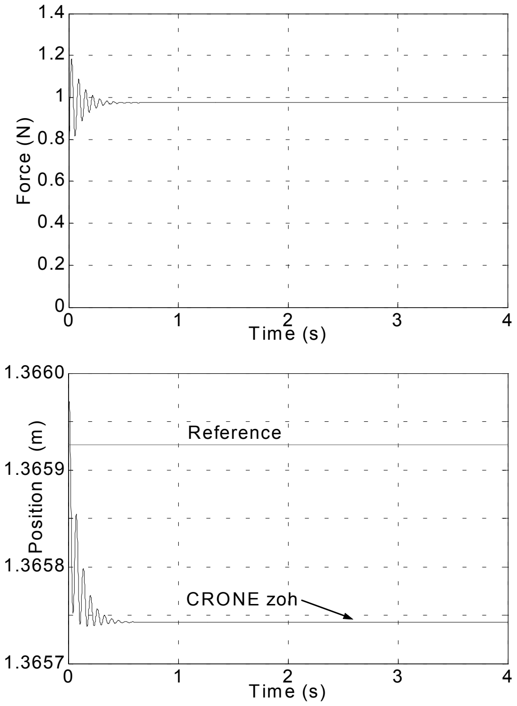

Figure 8. Performance of a discretised CRONE controller

Future work includes a more thorough study of formulas presented in Tables 2 and 3 (including for instance an analysis of zero and pole placement), and laboratory implementation of controllers simulated for the robotic arm.

Acknowledgements

This research was partially supported by programme POCTI, FCT, Ministério da Ciência e Tecnologia (Portugal), and ESF through the III Quadro Comunitário de Apoio.

Bibliography

[1] O. Khatib, "A unified approach for motion and force control of robot manipulators: the operational space formulation", *IEEE Journal of robotics and automation*. **3**, pp. 43-53, (1987).

[2] J. Machado, A. Azenha. Fractional-order hybrid control of robot manipulators. In 1998 IEEE international conference on systems, man and cybernetics: intelligent systems for humans in a cyberworld. [S.l.]: IEEE, 1998. 788-793.

[3] J. Machado. "Discrete-time fractional-order controllers", *Fractional calculus & applied analysis*. **4**, pp. 47-66 (2001).

[4] A. Oustaloup. La commande CRONE: commande robuste d'ordre non entier. Paris: Hermès, 1991.

[5] D. Valério, J. Sá da Costa. Time domain implementations of non-integer order controllers. In Controlo 2002. Aveiro: 5th Portuguese Conference on Automatic Control, 2002. 353-358.

[6] B. Vinagre. Modelado y control de sistemas dinámicos caracterizados por ecuaciones íntegro-diferenciales de orden fraccional. Madrid: Universidad Nacional de Educación a Distancia, 2001. PhD thesis.

[7] H. Wall. Analytic theory of continued fractions. Princeton: D. Van Nostrand Company, 1948.

Appendix: Remarks on tables

Formula (2) is easily proved by mathematical induction. No formal proofs were obtained for formulas (13), (14), (15) and (16), but they allow obtaining the corresponding series: a) up to the first eleven terms in their general expressions; and b) up to the 100th term for several particular values of *v*. Even though a proof cannot be replaced by such considerations, the precision obtained shall certainly exceed the one needed for any engineering implementation, since hardly more terms will be employed; and in several fields of Mathematics one must rely on considerations like those above (instead of formal proofs), since it is not possible, at least in the current state of knowledge, to validate results otherwise. Formulas (9) and (10) are obtained from expansions found, together with their proofs, in [87], pp. 335-346.

Formula	$G(s) = s^v \approx \dots$
1st order backward finite difference	$T^{-v}\left[0; \frac{1}{1}, \frac{vz^{-1}}{1}, \frac{-\frac{i(i+v)z^{-1}}{(2i-1)2i}}{1}, \frac{-\frac{i(i-v)z^{-1}}{2i(2i+1)}}{1}\right]_{i=1}^{n}$ (9)
Tustin	$\left(\frac{2}{T}\right)^v \left[1; \frac{2v}{-\frac{1}{z^{-1}} - v}, \frac{v^2 - i^2}{-\frac{2i+1}{z^{-1}}}\right]_{i=1}^{n}$ (10)
All other five formulas	Let *f*(*x*) be a real valued function given by the ratio of two polynomials: $f(x) = \frac{c_{10} + c_{11}x + c_{12}x^2 + c_{13}x^3 + \dots}{c_{00} + c_{01}x + c_{02}x^2 + c_{03}x^3 + \dots}$ Its continued fraction expansion is given by $f(x) = 0 + \frac{c_{10}}{c_{00} + \frac{c_{20}x}{c_{10} + \frac{c_{30}x}{c_{20} + \dots}}} = \left[0; \frac{c_{10}}{c_{00}}, \frac{c_{j+1,0}x}{c_{j,0}}\right]_{j=1}^{+\infty}$ $c_{j,i} = -\begin{vmatrix} c_{j-2,0} & c_{j-2,i+1} \\ c_{j-1,0} & c_{j-1,i+1} \end{vmatrix}$ (11)

Table 1. Continued fraction expansion formulas.

Formula	Obtained from	$G(s)=s^{v}\approx\ldots$
1st order backward finite difference	$s\approx\frac{1-z^{-1}}{T}$ or (1)	$\frac{1}{T^{v}}\left[\sum_{k=0}^{n}(-1)^{k}\frac{\Gamma(v+1)}{\Gamma(k+1)\Gamma(v-k+1)}z^{-k}\right]$ (12)
2nd order backward finite difference	$s\approx\frac{3-4z^{-1}+z^{-2}}{2T}$	$\left(\frac{3}{2T}\right)^{v}\left[\sum_{j=0}^{n}\frac{\Gamma(v+1)}{\Gamma(v-j+1)}\sum_{i=j}^{\min(2j;n)}\frac{(-1)^{i}z^{-i}(4/3)^{j}}{\Gamma(2j-i+1)\Gamma(i-j+1)4^{i-j}}\right]$ (13)
3rd order backward finite difference	$s\approx\frac{11-18z^{-1}+9z^{-2}-2z^{-3}}{6T}$	$\left(\frac{1}{6T}\right)^{v}\left[\sum_{i=0}^{n}(-1)^{i}z^{-i}\sum_{j=\mathscr{C}\left(\frac{i-1}{3}\right)+1}^{i}\frac{\Gamma(v+1)}{\Gamma(v-j+1)}11^{v-j}F_{ij}\right]$ (14)
	$F_{ij}=\frac{1}{\Gamma(i)}\sum_{k=\max\{0;i-2j\}}^{\mathscr{C}\left(\frac{i-j}{2}\right)}18^{j-k}E_{ijk}$,	$\begin{cases}E_{000}=1\\ E_{ijk}=\frac{i}{2j+k-i}E_{i-1;j-1;k}, \quad 2j+k>i\geq j+2k\wedge j>k\\ E_{3k;k;k}=12E_{3k-1;k;k-1}\\ E_{2j+k;j;k}=\frac{2j+k}{2(j-k)}E_{2j+k-1;j;k}\end{cases}$
Tustin	$s\approx\frac{2}{T}\frac{1-z^{-1}}{1+z^{-1}}$	$\left(\frac{2}{T}\right)^{v}\left[1+\sum_{j=1}^{n}\sum_{i=j}^{n}(-1)^{i}\frac{\Gamma(v+1)\Gamma(i)2^{j}z^{-i}}{\Gamma(v-j+1)\Gamma(j)\Gamma(i-j+1)\Gamma(j+1)}\right]$ (15)
Simpson	$s\approx\frac{3}{T}\frac{(1+z^{-1})(1-z^{-1})}{1+4z^{-1}+z^{-2}}$	$\left(\frac{3}{T}\right)^{v}\left\{1+\sum_{i=1}^{n}\left[(-1)^{i}z^{-i}\sum_{j=1}^{i}\frac{\Gamma(v+1)}{\Gamma(v-j+1)}C_{ij}\right]\right\}$ (16)
	Let $\mathscr{A}_{ij}$ be the set of all unordered sequences of *j* natural numbers adding up to *i*; let the s_{ij} be the sequences of $\mathscr{A}_{ij}$, $s_{ij}\in\mathscr{A}_{ij}$; and let $\mathscr{R}(s_{ij})$ be the product of the factorials of the numbers of times each natural appears in s_{ij}; that is to say, $\mathscr{A}_{ij}=\left\{(n_{1},n_{2},\ldots,n_{j}):n_{1},n_{2},\ldots,n_{j}\in\mathbb{N}\wedge\sum_{k=1}^{j}n_{k}=i\right\}$, $\mathscr{R}(s_{ij})=\prod_{n\in\mathbb{N}}(\text{number of times that } n \text{ appears in } s_{ij})!$ Then $C_{i1}=4^{i}+\sum_{j=1}^{\mathscr{C}\left(\frac{i}{2}\right)}4^{i-2j}(-1)^{j}\left[\binom{i-j}{i-2j}+\binom{i-j-1}{i-2j}\right]$, $C_{ij}=\sum_{s_{ij}\in\mathscr{A}_{ij}}\left(\frac{\prod_{\substack{n_{p}\in s_{ij}\\ p=1,\ldots,i}}C_{n_{p}1}}{\mathscr{R}(s_{ij})}\right)$, $1<j\leq i$	
Impulse response	$\mathscr{L}^{-1}\left[s^{v}\right]=\frac{t^{-v-1}}{\Gamma(-v)}$	$\left[\frac{T_{s}^{-v}}{\Gamma(-v+1)}-\frac{T_{s}^{-v-1}}{\Gamma(-v)}+\sum_{i=1}^{n}\frac{(iT_{s})^{-v-1}}{\Gamma(-v)}z^{-i}\right]$ (17)
Step response	$\mathscr{L}^{-1}\left\{s^{v}\times\frac{1}{s}\right\}=\frac{t^{-v}}{\Gamma(-v+1)}$	$\left(\sum_{i=0}^{n}a_{i}z^{-i}\right)$, $a_{0}=\frac{T_{s}^{-v}}{\Gamma(-v+1)}-\frac{T_{s}^{-v-1}}{\Gamma(-v)}$, $a_{k}=-\sum_{i=0}^{k-1}a_{i}+\frac{(kT_{s})^{-v}}{\Gamma(-v+1)}$, $k=1,2,\ldots,n$ (18)

Table 2. MacLaurin expansion formulas and time response formulas.

m_1=0.5 kg	r_1=1.0 m	$J_{1\text{m}}$=1.0 kg m^2	$J_{1\text{g}}$=4.0 kg m^2	M=0.03 kg	K=400 N/m
m_2=6.25 kg	r_2=0.8 m	$J_{2\text{m}}$=1.0 kg m^2	$J_{2\text{m}}$=4.0 kg m^2	B=1 Ns/m	θ=π/2 rad

Table 3. Robot parameters.